Project 079 Novel Noise Liner Development Enabled by Advanced Manufacturing

The Pennsylvania State University
RTX Technology Research Center
Altair Engineering
Cornerstone Research Group

Project Lead Investigator

Nicholas Meisel
Associate Professor
School of Engineering Design and Innovation
The Pennsylvania State University
University Park, PA 16802
nam20@psu.edu

University Participants

The Pennsylvania State University (Penn State)

- P.I.: Nicholas Meisel, Associate Professor of Engineering Design
- FAA Award Number: 13-C-AJFE-PSU-079
- Reporting Period: October 1, 2024, to September 30, 2025
- Tasks:
  1. Identifying Sensitivity of Acoustic Liner Performance to Key Design Variables
  2. Establishing Systematic Approach to Identify and Account for Manufacturing Error
  3. Automating the Generation of Acoustic Lattice Meshes

Project Funding Level

The ASCENT Project 079 received $1,200,000 from the Federal Aviation Administration (FAA) with match from Penn State ($110,000), RTX Technology Research Center ($450,000), Altair Engineering ($400,000), and Cornerstone Research Group ($240,000).

Investigation Team

The Pennsylvania State University

Nicholas Meisel (P.I.), Project management, task coordination, and student advising
Allison Beese (co-P.I.), Student advising, Tasks 1 and 2
Eric Greenwood (co-P.I.), Student advising, Task 1
Alden Packer (graduate student; PhD), Task 1
Joeseph Windows (graduate student, MS), Task 2

RTX Technology Research Center (RTRC)

Jeff Mendoza (P.I.), Project coordination and management at RTRC
Julian Winkler (co-P.I.), Acoustic analysis and evaluation as part of Task 1
Aaron Reimann (co-P.I.), Acoustic analysis and evaluation as part of Task 1
Kenji Homma (investigator), Acoustic analysis and evaluation as part of Task 1
Paul Braunwart (investigator), Acoustic analysis and evaluation as part of Task 1

Altair Engineering (Altair)

Eric Nelson (P.I.), Manufacturability accommodation as part of Task 2

Cornerstone Research Group (CRG)
Akiva Wernick (P.I.), Direct mesh generation as a part of Task 3

Project Overview

Penn State in collaboration with industrial partners, RTRC, Altair, and CRG, along with government collaborator, the National Aeronautics and Space Administration (NASA) Langley Research Center (LaRC), will help the FAA develop and advance innovative engine acoustic liner technology to meet the demands of low noise for future aircraft. Specifically, the team will develop and demonstrate a method to rapidly design, manufacture, and evaluate novel structures that enhance noise attenuation in aircraft engines. Analysis and experimental testing will be used to characterize the effect of lattice topology, geometry, and features size to attenuate noise while ensuring the manufacturability of these complex structures in different materials. Advanced manufacturing technologies will be used to enable rapid design-build-test cycles for liner development, including assessment of structural integrity and acoustic performance. Promising engine liner designs and their performance will be documented to aid future advancements in aircraft engine noise reduction.

The overall project approach includes the following steps:

1. Establish a set of acoustic requirements for future aircraft engine designs.
2. Design and analyze lattice-based acoustic liners using advanced software tools.
3. Perform rapid, iterative prototyping and testing to identify promising designs and materials.
4. Conduct detailed assessments of manufacturability.
5. Perform acoustic and structural evaluations of novel liners in collaboration with NASA LaRC.
6. Document results and archive data for the FAA.

Task 1 – Sensitivity of Acoustic Liner Performance to Key Design Variables

The Pennsylvania State University, RTX Technology Research Center

Objective

The objective of this task is to identify the sensitivity of the additive manufacturing (AM) acoustic liner designs to changes in key design parameters. This sensitivity will be compared against traditional honeycomb-shaped liners.

Research Approach

To verify the viability of triply periodic minimal surface (TPMS) lattice-based acoustic liners, they were compared against traditional single degree-of-freedom (SDOF) and double degree-of-freedom (DDOF) liners. Allowing for an equal comparison, both categories of liners were first optimized using the same target objective, that of maximizing acoustic absorption in defined frequency ranges. The design optimization process that was used was created through the unification of necessary pieces of software that performed the functions of parameterizing the design variables for the acoustic liner concepts, modeling the geometries, simulating the acoustics physics, and analyzing the response objectives.

Parameterization of Design Variables

For SDOF, DDOF, and TPMS based liners alike, optimization requires that the available design variables be parameterized and given bounds within which to explore. For each liner type, and subsequent construction, there are changes to the design that can impact the acoustic response of the liner. For all liner types in this study, the total depth or thickness of the liner was capped at 1.5 in. or 38.1 mm, to compare the performances of the lattices when similarly constrained. The design parameters of the facesheet were also given equal constraints across all lattice types.

The SDOF acoustic liner has four main design variables, shown in Figure 1. Three of the parameters correspond to properties of the perforated facesheet, percent open area (POA), facesheet thickness, t, and perforation diameter, d. To eliminate the possibility of the POA and perforation diameter requiring a non-whole number of perforations, the number of perforations was used as a design variable, and the POA was calculated from the number of perforations multiplied by the area of a single perforation, all divided by the total area of a cell. That POA value was then used in modeling. The depth of the honeycomb core, D, pertains to the honeycomb core itself, and is a critical parameter for resonating liners, like the SDOF. Varying the depth of the liner adjusts the frequency where the most absorption will occur, with deeper liners corresponding to lower frequency absorption. The facesheet parameters also affect the acoustic response by creating resistive losses through friction in the perforations. DDOF acoustic liners maintain the same design variables as the SDOF liner, but the added intermediate septum introduces additional variables that can be altered to achieve higher acoustic

absorbing performance. Like the facesheet in the SDOF, the DDOF facesheet also causes acoustic energy losses through friction within the perforations. This is added to by the perforations in the intermediate septum. The lowest frequency response of the DDOF liner is still driven by the total depth, as with the SDOF; however the septum can cause additional ranges of high absorption. This dividing septum has thickness, t_s, and variable permeability properties, such as percent open area, POA_s, and perforation diameter, d_s. The depth of the septum within the honeycomb core, D_s, can be varied as well, yielding in total three additional design variables. Figure 1 shows the honeycomb core liner with the additional septum related design variables included.

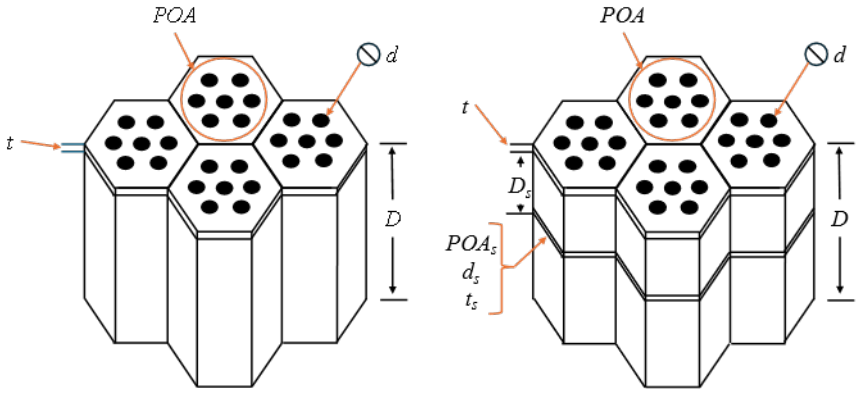

Figure 1. Single degree-of-freedom (SDOF) and double degree-of-freedom (DDOF) liner designs with relevant design variables: liner depth (D), facesheet thickness (t), facesheet perforation diameter (d), percent open area (POA), septum depth (D_s), and percent open area and perforation diameter of the septum (POA_s and d_s).

Instead of a cavity with variable depth, TPMS lattice structures encompass a complex pair of channels with unique tortuous paths that are controlled by specific design variables. The design variables used in this study are general to all TPMS lattices, but the lattice types of Schwarz P and Diamond were selected for exploration and comparison with the SDOF and DDOF. Schwarz P was selected for the study based on the research team's previous preliminary investigations, while the Diamond lattice was selected for its high levels of internal tortuosity. The first group of design parameters is the variability of unit cell size. This allows us to adjust the size of individual unit cells in three directions, X Y, and Z, effectively stretching or compressing the cells of the lattice in those directions (see Figure 2). These variables can also be scaled uniformly to vary the overall size of the unit cell. Due to the symmetry inherent in normal incidence testing, the unit cell size in X and Y were coupled, and the samples were modeled in a 1x1xn stack of cells. The total depth of the sample was determined by the height of the cells (Z) multiplied by another design variable, the total number of cells in the Z-direction. These design variables modify the internal volumes of the lattices, potentially causing variations in the resonating effects of the geometry.

Control of the levelset or iso-surface offset of TPMS lattices allows for the offsetting of material from the surface midplane to either side of the surface. This effect is shown in Figure 2 for both the Schwarz P and Diamond lattices. TPMS lattices split a region into two non-intersecting sub-regions. Changes in levelset varies the volumes of the two sub-regions, expanding one while contracting the other, promoting a unique acoustic response in each region. These two subregions can be broadly differentiated as the endo-region and the exo-region. In this study, levelset was defined twice, once at the facesheet and once at the backplate. This causes a functional grading effect of the levelset, where cells of the lattice in the Z-direction can have different levelset values.

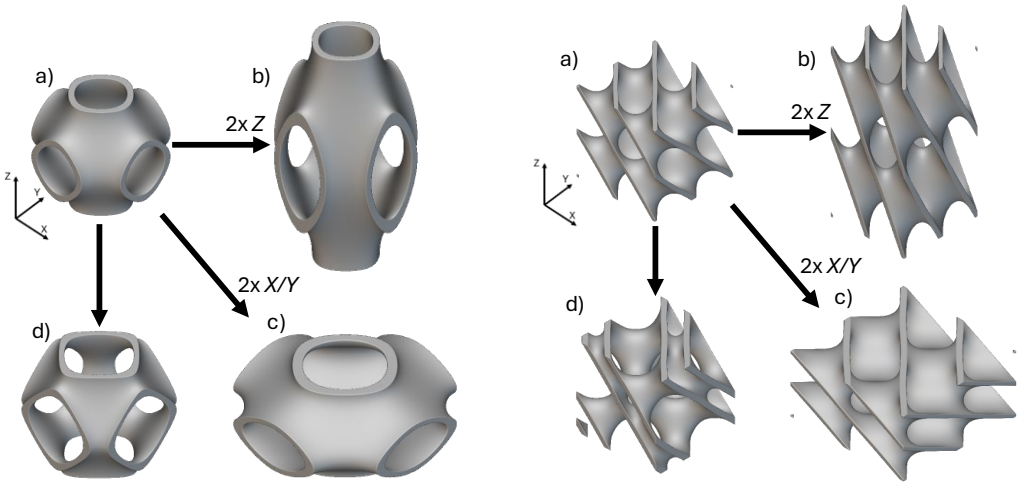

Figure 2. Triply periodic minimal surface (TPMS) lattice variations from the basic unit cell (a) for the Schwarz P and Diamond lattices (left and right, respectively), (b) change in Z height, (c) change in X/Y width, and (d) change in levelset.

The additional benefit of the presence of the two sub-regions is that a unique facesheet can be applied to each region separately. In this way, each region essentially acts as its own acoustic liner, leading to the possibility of wider ranges of high absorption. For both the endo and the exo-regions, the design variables of perforation diameter and number of perforations can be defined uniquely. Examples of the facesheet over Schwarz P and Diamond unit cells are shown in Figure 3. Variation of the facesheet thickness is consistent between the two regions to avoid off-setting either the top of the facesheet or the back of the lattice. This configuration leads to five design variables for the TPMS facesheet alone, in addition to the five variables from the lattice core geometry. A summary of the available design variables associated with each liner in the current study provided in Table 1.

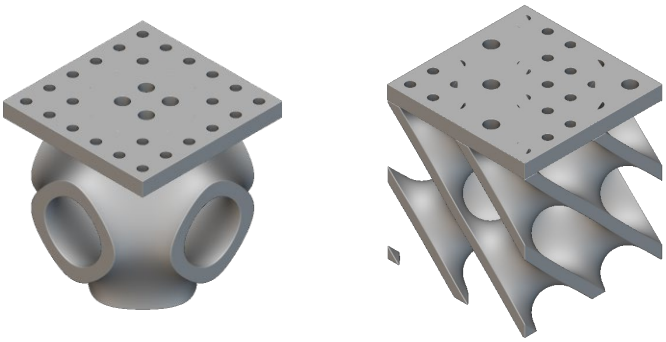

Figure 3. Facesheet depictions for the Schwarz P (left) and Diamond (right) triply periodic minimal surface (TPMS) lattice geometries. For these examples, the endo-region has a larger perforation diameter than the exo-region.

Table 1. Design variables of the single degree-of-freedom (SDOF), double degree-of-freedom (DDOF), and triply periodic minimal surface (TPMS) acoustic liners.

SDOF	DDOF	TPMS
# of Facesheet Perforations **Perforation Diameter**	# of Facesheet Perforations Perforation Diameter	X/Y Unit Cell Size Z Unit Cell Size
Facesheet Thickness **Liner Depth**	Facesheet Thickness Liner Diameter	Z: # of Cells Level set (Facesheet)
	# of Septum Perforations	Level set (Backplate)
	Septum Perforation Diameter Septum Thickness	Facesheet Thickness Endo Perforation Diameter
	Septum Depth	# of Endo Perforations Exo Perforation Diameter
		# of Exo Perforations

Geometry Modeling and Acoustic Simulation

The next step in the process is to represent the liner geometry in a way that we can parameterize the important geometric components and calculate the acoustic performance. For the SDOF and DDOF acoustic liners, the Zwikker-Kosten Transmission Line (ZKTL) method was used to model geometry and predict acoustic performance. In this method, each section of the liner is represented by a transmission matrix, including both cavities and perforated sheets. For modeling of the perforated sheets, the flow resistance is calculated using the lumped element model or two parameter model, shown in Equation 1. In this equation, ζ represents the impedance, ϑ represents the acoustic resistance (linear and nonlinear), and χ represents the acoustic reactance of the facesheet. It is referred to as the two-parameter model because it breaks the acoustic resistance into two terms: the linear and the non-linear resistance. This model is suitable for calculating the acoustic response of SDOF acoustic liners directly, but it was implemented into the ZKTL code in order to be robust enough to also predict DDOF performance.

$$\zeta = \theta + i\chi = \theta_{lin} + \theta_{nonlin} + i\chi_{fs} \quad \text{(Eq. 1)}$$

The tradeoff of exploring higher complexity geometries is that analytical solutions often do not exist to model the physics present in these structures. Because of this, a numerical approach is necessary. First, the acoustic liner structure must be modeled in computer aided design (CAD) software, then a mesh will be applied to the geometry, and a numerical simulation of the physics will be applied to the mesh. For the TPMS acoustic liners, an implicit geometry CAD software, nTopology, was used to generate the lattice geometries. As an implicit geometry software tool, nTopology is able to model mathematically defined functions and efficiently represent and export the complex lattice geometry. The lattice geometry files from nTopology were then imported into COMSOL Multiphysics® software (COMSOL). Additionally, select SDOF and DDOF designs were modeled in CAD and simulated in COMSOL for verification of the previously discussed analytical approach. Geometry generation of liner designs was performed on local desktop machines, but COMSOL was run on a cluster computing cloud service through Penn State. The pressure acoustics COMSOL library was used to apply the necessary boundary conditions for modeling acoustic performance. All walls in the model were treated as hard wall boundaries, and a perforated plate boundary condition representing a perforated facesheet was used to reduce the computation time caused by attempting to mesh such small features as the facesheet perforations. The facesheet design variables were imported into the study and applied to this boundary condition. A physics-defined mesh was used, which automatically adjusts the element size according to the physics being simulated. The acoustic response is solved across a prescribed frequency range of 300 to 3,400 Hz, which are the lower and upper bound of viable frequencies of typical normal incidence tube experimental testing. After the acoustic data are gathered, the response objectives are extracted for performance characterization.

The two main pieces of information that are output from both numerical and analytical acoustic modeling are acoustic resistance, ϑ, and reactance, χ. For every tested frequency, these values describe the resistance to sound flow due to friction and heat, and to inertia of the medium, respectively. Those two quantities can be used to calculate the acoustic

® COMSOL Multiphysics is a registered trademark of Comsol AB, Stockholm, Sweden.

absorption coefficient, α, which is the response objective used in the optimizations. Acoustic absorption coefficient is calculated as follows for normal incident acoustics.

$$\alpha = \frac{4\theta}{(1+\theta)^2+\chi^2} \quad \text{(Eq. 2)}$$

The acoustic absorption coefficient is an efficient performance metric, providing a value between zero (complete reflection) and one (complete absorption) for each frequency. When plotted, the result is an acoustic absorption curve. When calculating acoustic absorption for an acoustic liner design, the result is a series of absorption values for every frequency in the range that is tested. This poses difficulty when comparing the performance between two or more liners because it becomes inefficient to compare the absorption at every frequency. The most efficient metric would be a single scalar value to describe the general performance of the acoustic absorption coefficient in the desired frequency range. The method used to provide this metric is to integrate the absorption coefficient curve over a predetermined bandwidth, yielding a single value describing the absorption performance. This can be done for both the entire sample bandwidth as well as smaller sub-bands. Where our simulations tested over a frequency range of 300 to 3,400 Hz, the absorption objectives of broadband (300 to 3,400 Hz), low band (300 to 1,300 Hz), mid band (1,300 to 2,300 Hz), and high band (2,300 to 3,400 Hz) were used in four distinct optimizations.

Optimization Approach

With design and simulation capabilities established and demonstrated, the optimization process was run through the design exploration and automation software, Altair HyperStudy.® HyperStudy was used as the interface for parameterizing the design variables of the liner geometries and creating the design exploration routine. It was linked to nTopology and was able to autonomously generate TPMS acoustic liner designs. However, due to the use of COMSOL being used on a remote server, direct automation between HyperStudy and COMSOL was not available. Therefore, large, spacing-filling design of experiments (DOE) were established to generate many TPMS lattice geometries at once. Then, all the designs were uploaded to the COMSOL server where a batch script automation process was set up to iteratively simulate each design. When all designs were simulated, the acoustic results were imported back into HyperStudy for analysis.

The traditional liners followed the same optimization approach as the TPMS designs, with the exception of the geometry and physics being modeled in a python script instead of nTopology and COMSOL. Not needing the same computational power as the finite element solver, the ZKTL python script was run for the entire DOE on a local desktop machine, and results were imported immediately back into HyperStudy. Verification using the COMSOL method was performed on select samples to ensure that the ZKTL code and initial search were providing usable results. The verification showed that the ZKTL script was accurate at low frequencies, but diverged slightly at higher frequencies, underpredicting the acoustic absorption. Because this underprediction was consistent across all samples, the ZKTL method was used to identify an estimation of acoustic performance, while COMSOL provided a higher fidelity solution.

Results and Discussion

Using the described process, SDOF, DDOF, Schwarz P, and Diamond acoustic liners were optimized for acoustic absorption in four target frequency bandwidths: (1) broadband (300 to 3,400 Hz), (2) low band (300 to 1,300 Hz), (3) mid band (1,300 to 2,300 Hz), and (4) high band (2,300 to 3,400 Hz). DOE datasets were created for both TPMS-based liners, Schwarz P and Diamond, and traditional liners, SDOF and DDOF. 500 samples were generated for each TPMS-based liner and each traditional liner, from which the top performing designs would be selected for each lattice type. The simulation of each batch of lattice samples was done over the course of several days on the Penn State cluster computer due to the approximately 10-min solution time for each sample. The ZKTL code for the traditional liners was much faster, solving all 500 samples in approximately 10 min on a local machine. Using the design exploration dashboard from previous work, the liner design concepts, with accompanying performance metrics, were sorted according to the response objectives of acoustic absorption over various frequency bandwidths. For each response objective and each liner type, the liner concept with the highest performance was identified.

For the traditional liners, after the highest performing liner designs were identified, they were modeled and simulated in COMSOL for verification. The coplotted ZKTL and COMSOL results are shown in Figure 4. The results of the two simulation methods predict similar trends in the absorption coefficient curves, though at frequencies greater than 1,600 Hz, the COMSOL solution predicts higher absorption. This is less evident in the SDOF designs, which align very well in all cases

® HyperStudy is a registered trademark of Altair Engineering, Inc., Troy, Michigan.

except for the high band target. Because the COMSOL solution comes from a higher fidelity solver than the ZKTL solution, the comparisons with the TPMS liners were made using the COMSOL results. This also helps to ensure consistency within analysis and optimization.

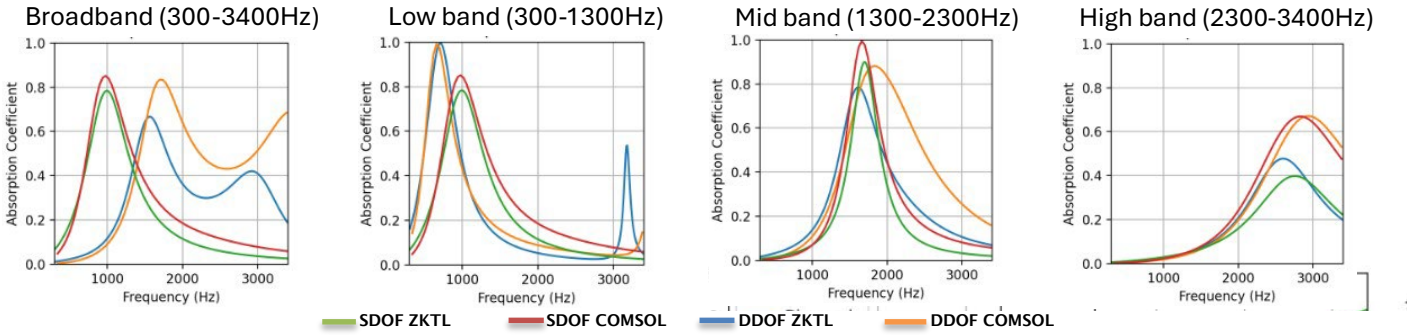

Figure 4. Single degree-of-freedom (SDOF) and double degree-of-freedom (DDOF) samples compared using Zwikker-Kosten Transmission Line (ZKTL) and COMSOL solutions.

When looking at the images of the generated, optimized liner designs in the design exploration dashboard, trends were more easily noted in the SDOF and DDOF liner types than in the TPMS designs. For example, the trend for traditional liners total thickness (depth for the SDOF and the sum of two depths for the DDOF) led to deeper liners being better adapted to low frequencies and shorter liners being better adapted to high frequencies. However, a more nuanced assessment was revealed using a sensitivity analysis. The sensitivity analysis on the DOE results from the SDOF and DDOF liners showed that the facesheet parameters, perforation diameter and the number of perforations, had some of the greatest impact across all target frequency bandwidths. Perforation diameter of the facesheet (as opposed to the septum) was consistently one of the most impactful design variables for the traditional liners. The facesheet was also highly impactful in the TPMS liner response, though the key design parameter differed between the Diamond and Schwarz P. For the Diamond lattice, the number of perforations in both the endo and exo regions were highly impactful; the perforation diameters remained important, but *X/Y* unit cell size and number of stacked unit cells were more impactful across all target ranges. The two most impactful design variables for the Schwarz P liners were the exo region facesheet perforation diameter and number of perforations. This makes intuitive sense because the structure of the Schwarz P unit cell already restricts the available open area of the endo region. For both Schwarz P and Diamond, in the high band target bandwidth, the number of stacked unit cells was the most impactful design parameter. Because the number of cells directly influenced the total height of the liner, and high frequency absorption favors shorter channels, this design parameter was critical for the high band regime.

With trends in the lattice geometry noted, the comparison results for liner performance are shown in Figure 5, where for each target frequency range, acoustic absorption coefficient is compared for the four liner types. In each of the target frequency bands, the TPMS acoustic liners had similar or better performance than the traditional liners; for example, in the broadband regime, the DDOF response value was 933 Hz while the Schwarz P design had the value of 1,372 Hz. For the broadband target, SDOF peaked at a lower frequency than DDOF, Schwarz P, or Diamond; however, the absorption of the DDOF and TPMS designs acted across a wider frequency range, with the Schwarz P design showing the widest band. The low band target showed comparable results for all four liner types, all very high absorption coefficients at a peak frequency around 900 Hz. The mid band target also showed a cluster where all liners peaked around 1,850 Hz, except the Schwarz P design also had an additional absorption peak at lower frequencies. Finally, in the high frequency target band, the TPMS designs showed higher absorption than the traditional liners.

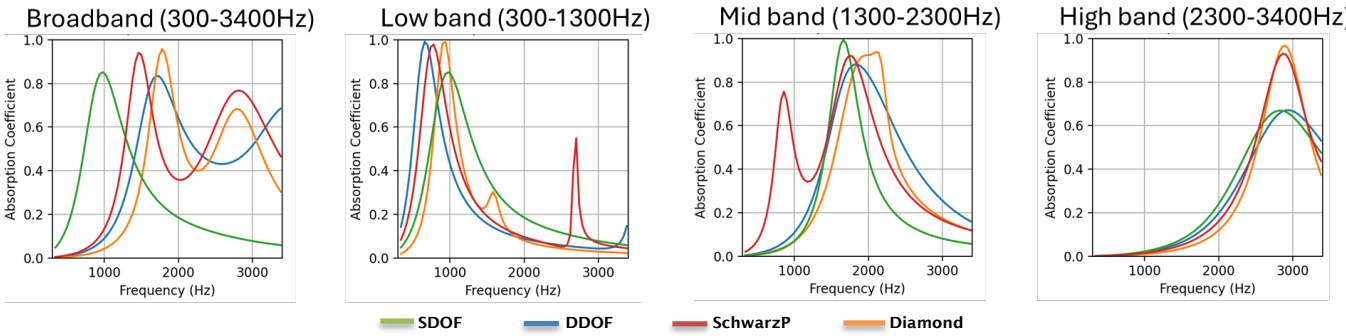

Figure 5. Acoustic absorption coefficient plots comparing four acoustic liner types, across four target frequency bands.

In the four target frequency ranges, the SDOF and DDOF acoustic liner types converged on designs that yielded similar performance. The intermediate perforated septum in the DDOF liner should produce a higher performance liner; however, all liners were subject to a maximum thickness constraint, which may have impeded the DDOF from taking full advantage of the perforated septum. Looking at the liner the total depth of all the liners (displayed in Table 2), the Schwarz P and Diamond acoustic liners required less height than the traditional liners to achieve competitive low and broadband acoustic absorption performance. This suggests that using greater design freedom, such as with AM enabled TPMS lattice acoustic liners, performance of traditional acoustic liners can be matched, while requiring less volume within the nacelle.

Table 2. Depth (mm) across all candidate liner types. DDOF: double degree-of-freedom; SDOF: single degree-of-freedom.

Liner Type	Broadband Depth (mm)	Low Band (mm)	Mid Band (mm)	High Band (mm)
SDOF	36.0	36.0	7.3	11.0
DDOF	21.4	37.0	36.6	14.5
Schwarz P	11.9	27.1	16.0	12.5
Diamond	11.6	18.7	13.0	9.5

The absorption curves of the Diamond and Schwarz P liners show two peaks in all target ranges except the high band. In the broadband regime, the DDOF design mounts to what would be an additional peak, but that peak is out of range. In the DDOF, the second peak is achieved through the perforated septum and the resonating effects of having two depths (from facesheet to septum, and from facesheet to backplate) creates two peaks. Due to the total depth constraint, the second peak is often out of the test range. For the TPMS lattices, there is only one depth to the structure, though the path is potentially more tortuous. The second peak, in the case of these lattices, comes from the endo and exo regions. The facesheets over the two regions, in addition to differences in the internal channel, create an additional peak. Because the depth is constant, the second peak is largely controlled by the facesheet parameters, so the two peaks are able to appear closer together. This is likely the cause of the mid band Diamond lattice behavior, where the peak plateaus before descending. This is a useful phenomenon when trying to absorb noise are two frequencies that are in close proximity to one another.

Milestones

- Demonstrated the use of the HyperStudy dashboard across traditional and TPMS liners.
- Cemented the benefits of TPMS liners in acoustic absorption.
- Initialized sensitivity study of TPMS liners, to be further expanded in-depth.

Major Accomplishments

- Applied theoretical and computational analysis to SDOF and DDOF liner specimens.
- Compared computational performance of optimized TPMS liners against traditional liners.
- Identified performance advantages of TPMS liners, especially as related to required liner thickness.

Publications

Packer, A., Reimann, C. A., Winkler, J., Homma, K., Mendoza, J., Greenwood, E., Manahan, M., & Meisel, N. A. (2025) Evaluating the Performance of Novel TPMS-Based Acoustic Liner Designs Suitable for Additive Manufacturing. *Proceedings of the Annual International Solid Freeform Fabrication Symposium*, in press.

Outreach Efforts

None.

Awards

None.

Student Involvement

One graduate student was involved in this task. Alden Packer, a PhD student in mechanical engineering who worked closely with RTRC to refine the modeling and sensitivity analysis of the acoustic liners.

Plans for Next Period

Focus on validating this sensitivity in experimental specimens with initial design sensitivity identified at the computational level. This will enable a robust understanding of the design science underpinning the creation of high-performing acoustic liners via AM.

Task 2 – Systematic Approach to Identify/Account for Manufacturing Error

The Pennsylvania State University, Altair Engineering

Objective

The objective of this task is to identify, measure, and account for the presence of manufacturing variations and defects in TPMS liners created via vat photopolymerization AM.

Research Approach

This section explores a pipeline for rapid cost-efficient analysis of defects and stochastic errors in manufactured acoustic liners without the need for extensive resources involved in current inspection methods like x-ray computed tomography (XCT). The method is designed to screen for surface level defect and dimensional accuracy but is not intended for full three-dimensional (3D) part inspection. It uses a combination of manual measurements and image processing tools to find the average manufactured deviation in the printed liners. From these measurements, approximate distributions can be found for the printed variation of the liner design variables.

Overview of Liner Design and Manufacturing

To allow for the removal of excess resin in the lattice core of the acoustic liner used in this paper, the liner is printed as two pieces and assembled after printing. The two parts are referred to as the liner casing and the liner core as shown in Figure 6. The liner casing acts as the housing for the liner core to slot into. The liner core consists of a TPMS Schwarz-P lattice structure connected to a perforated face sheet. A Schwarz-P lattice is chosen because it was found to have promising acoustic performance during preliminary tests. The liner core is modeled using nTop for the lattice structure and SOLIDWORKS® for the perforated face sheet. nTop requires lattice design parameters for both the overall bulk structure and the individual unit cell being tessellated throughout space. The design parameters of the bulk lattice are primarily dictated by the acoustic testing rig (in this case a normal incidence tube) since the active area of the liner needs to align with the active area of the test rig. The unit cell and face sheet design parameters can be varied based on the desired performance of the liner and are the main drivers behind the acoustic performance of the specimen. The face sheet is designed to be a flat solid sheet with a user specified perforation pattern that aligns with the lattice underneath. Once the face sheet is designed in SOLIDWORKS, it is exported as a Parasolid and imported into nTop where it is attached to the top of the lattice to form a single implicit body. The single body is then exported as a .3MF mesh for manufacturing.

® SOLIDWORKS is a registered trademark of Dassault Systemes Solidworks Corporation, Waltham, Massachusetts.

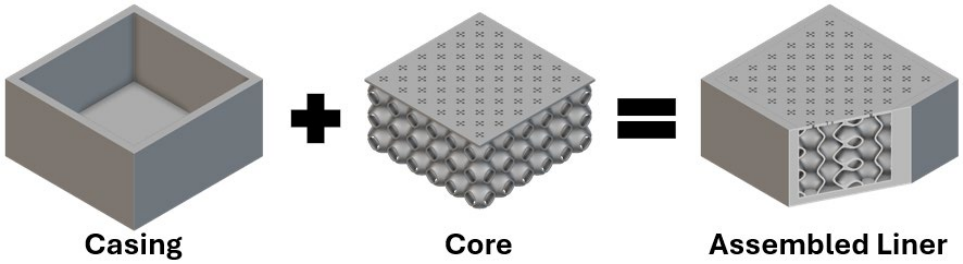

Figure 6. Acoustic Sample Design.

The liner core is printed on a Form 4® resin printer which uses masked stereolithography (MSLA). The core is prepped by importing the mesh in PreForm® where it is carefully oriented with a 20° tilt about the y-axis, supported, and sliced for printing. For acoustic purposes, the liner is required to be printed in a rigid material. The chosen resin also needs to be opaque so that the features of the part are visible for image detection. To ensure proper resin evacuation after printing, the part is washed once upside down and once right-side up in a FormWash™ station. With the excess resin removed, the part is cured in a FormCure™ station. Support material is then removed from the part, and it is ready for inspection.

Manual Measurement Method

The inspection pipeline in this report focuses on capturing stochastic variability through a combination of both manual measurements and two-dimensional image inspection. One of the most limiting factors with this approach is that, since a significant portion of the lattice in the liner core is enclosed by the outermost layer of Schwarz-P lattice cells and the face sheet, it is not possible to measure the internal lattice structure. Because of this, assessment must be based on the assumption that measurements from the external lattice bulbs and face sheet are representative of the entire liner core. Unfortunately, this assumption limits the accuracy of the measurement approach since there is no easy way to verify that the internal bulbs of the lattice share the same geometry as the outer surfaces.

There are several design variables that define the acoustic liner core and impact the acoustic properties. The overall length and width of the core are dictated by the testing apparatus and are not included as a design variable since they are considered fixed. The face sheet is defined by thickness, perforation diameter, and POA. The lattice is defined by a unit cell size, a wall thickness, and an isovalue. Measurements that can be taken manually using digital calipers (NEIKO® 01407A) include the face sheet thickness, the unit cell size, and the wall thickness as shown in Figure 7. The face sheet thickness is measured around the edge of the face sheet where the lattice bulbs join the face sheet and in between two lattice bulbs. The unit cell size is found by measuring the distance from the edge of a wall on one cell to the same edge on an adjacent cell. The wall thickness is found by measuring thickness of the walls at the pore openings. To account for the different print resolutions in the X-Y and Z directions on the Form 4 printer, the cell size and wall thickness measurements are grouped based on their orientation and location. Measurements taken on the sides (3 by 9 unit cell planes) along the length are considered “side length measurements” while measurements taken along the depth of the sides are considered “side depth measurements.” Additionally, measurements from the cells making up the 6x6 bottom of the core, defined as “bottom length measurements,” are kept separate due to the increased number of support structures that get attached to the bottom during printing. The removal process of such support material may cause bumps, chips, or cracks in the walls of the lattice which can affect the quality of the measurements around the locations where support structures are attached. Due to the 20° tilt used for manufacturing the sample, x-, y-, and x-axis of the printed core do not perfectly align with the axes of the printer; however, the X-Y and Z dimensions of the core should still be primarily impacted by the corresponding X-Y and Z resolutions of the printer.

® Form 4 is a registered trademark of Formlabs Inc., Somerville, Massachusetts.
® Preform is a registered trademark of Formlabs Inc., Somerville, Massachusetts.
™ FormWash is a trademark of Formlabs Inc., Somerville, Massachusetts.
™ FormCure is a trademark of Formlabs Inc., Somerville, Massachusetts.
® NEIKO is a registered trademark of Ridgerock Tools, Inc., Corona, California.

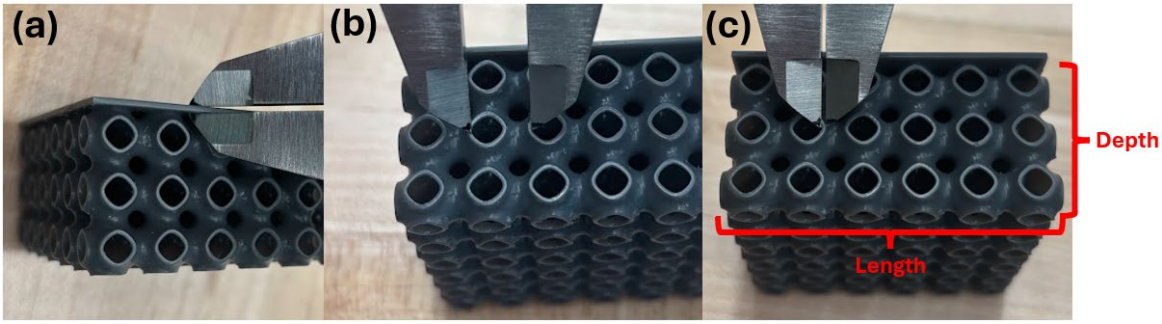

Figure 7. Measurement technique for (a) the face sheet thickness, (b) the unit cell size, and (c) the wall thickness.

In addition to parameters that are measured manually, the perforation diameter, POA, and isovalue are also measured. Since these parameters are too small to accurately measure with standard digital calipers, they are instead measured using a combination of several image processing tools. To accomplish this, it is necessary to first capture images of the sample from multiple views; this can be accomplished using a standard Apple® iPhone® 15 back camera to photograph the face sheet, sides, and bottom of the liner core. The images are then imported into Adobe® Lightroom® where a lens correction is applied (Apple iPhone 15 back camera 5.96mm f/1.6) and the image is cropped to remove the excess background around the liner core. Additionally, perspective correction is applied to address any camera tilt and remove the remaining pin cushion distortion, bringing all the opposing edges parallel to each other. This process results in images of the core where the exposed sides match the physical part as much as possible. After editing, the images can be used for inspection. To capture the perforation diameters and POA, the face sheet image is imported into the analysis tool ImageJ. The measurement scale is set, and the image is further cropped to only capture the area of the face sheet where the perforations are found. The image is then thresholded up to the point immediately before any of the perforations start to fade away. After removing any noise in the image due to artifacts such as layer lines, ImageJ's particle analysis tool is used to capture the individual areas of the face sheet perforations. Since the perforations in the face sheet are not perfectly circular, the effective diameter is estimated using their area. In some cases, excess resin or other contaminants can cause perforations to become partially blocked. Additionally, some of the residual noise particles in the image may be detected as very small areas. To remove the impact of the blockages and noise particles, any estimated diameter less than 80% of the nominal design diameter is removed from the data. This process yields a dataset of as-printed estimated perforation diameters. To estimate the POA, the area of all the particles in the thresholded image are combined and divided by the total measured area of the face sheet.

The final value to measure is the isovalue. The main purpose of the isovalue is to control the volume ratio between the endo and exo void channels. This means that the isovalue also controls the ratio of cross-sectional area between the two channels. Unfortunately, since the isovalue is a somewhat arbitrary constant when defining lattice geometry, measuring it can be difficult. For a Schwarz-P lattice, changing the isovalue changes the cross-sectional area ratio between the endo and exo pores as shown in Figure 8. To find the ideal relationship between the isovalue and the cross-sectional area ratio of the pores, images of nTop models at different isovalues are carefully thresholded, cropped, and cleaned so that the area ratio of the pores, in pixels, can be used to establish a correlation with the isovalues. With this relationship, the as manufactured isovalue can be estimated by finding the ratios of the endo and exo pores in the printed core. First, the edited images of the core sides and bottom are run through a Canny edge detection algorithm. This is necessary because the threshold function of ImageJ cannot accurately capture the lattice pores due to the uneven lighting in the images. Unwanted edges inside of pore areas are then removed and any small gaps in the pore edges are closed. Area ratios are then captured between each endo and corresponding exo pore. Finally, the as manufactured isovalues are determined based off the isovalue/area relationship established previously.

® Apple and iPhone are registered trademarks of Apple Inc., Cupertino, California.
® Adobe and Lightroom are registered trademarks of Adobe Inc., San Jose, California.

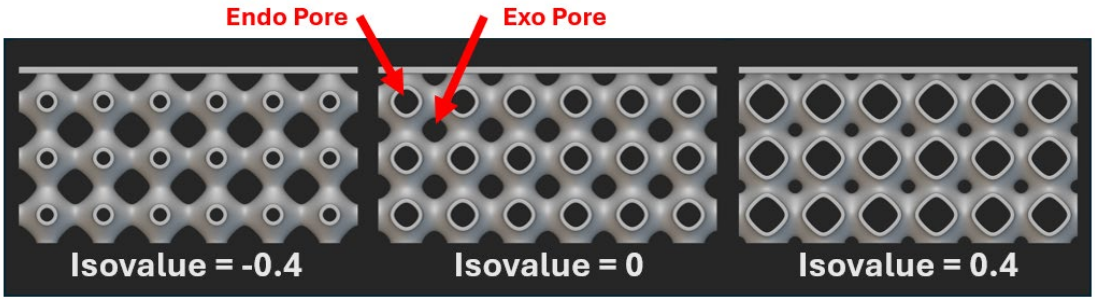

Figure 8. The effect of the isovalue on the cross-sectional area of the endo and exo lattice pores.

To capture the manufacturing deviation from the nominal design, each of the design variables is measured to find the average manufactured value and the standard deviation when possible. Crucially, several of these design parameters can be measured in multiple locations to create distributions that can be visually interpreted through the use of histograms or other means. A summary of each measured parameter is provided in Table 3. While the proposed approach intends to be systematic and as consistent as possible, some of the measurement techniques can still be somewhat subjective in nature. For example, due to uneven lighting, the user may be required to make a judgement call for what degree to threshold the face sheet perforation images. Face sheet perforation measurements could be verified using a second measure such as a pin gauge. The use of the calipers can also cause slight variations in the measured data. Since the calipers are harder than the resin, increasing the clamping pressure can compress the resin leading to smaller measured thickness values. The unit cell size measurements can also vary since the user has to do their best to properly align the calipers to the pore edges of the unit cell pores. Finally, the editing conducted on the photo could lead to changes in the interpretation of the printed geometry which could reflect in the final data.

Table 3. An overview of the parameters measured for a Schwarz-P liner core.

Measurement Tool	Parameter	Measurement Technique
Digital calipers	Face Sheet Thickness	Measure the thickness around the edge of the face sheet.
	Unit Cell Size	Measure the offset unit cell size by finding the distance from the pore edge of one cell to the corresponding pore edge of an adjacent cell.
	Wall Thickness	Measure the wall thickness around the exposed lattice pore edges.
Image processing and analysis	Perforation Diameter	Threshold images of the face sheet so that only the perforations are visible and then batch measure the areas of the perforations. Use the areas to estimate the effective diameter of each perforation.
	Percent open area	Threshold images of the face sheet so that only the perforations are visible and then find the total area of the perforations. Divide the total perforation area by the total area of the face sheet.
	Isovalue	Use edge detection to capture clean edges of the endo and exo lattice pores. Find the cross-sectional area ratio between the corresponding endo and exo pores. Convert the ratios to isovalues using an isovalue vs. area ratio relationship calculated from the ideal model.

Test Liner Core Design

The first step in demonstrating the defect detection pipeline was to develop a representative acoustic liner core. The core used for this case study was designed with both a length and width of 50.8 mm based on a normal incidence tube to be used for later testing. While these dimensions are not a focus of our error identification, they will be important for measuring the manufactured POA of the sample. The parameters used to design the face sheet included a face sheet thickness of 1 mm, perforation diameter of 0.8 mm, and a POA of 5.94% which was dictated by the perforation pattern of the face sheet. The TPMS Schwarz-P lattice was designed with a uniform wall thickness of 0.6 mm, unit cell size of approximately 8.47 mm, and an isovalue of 0.2. The final printed core is shown in Figure 9 both with and without supports

attached. The core was printed in Form Tough 2000 resin at a layer height of 0.05 mm. It was then washed in the Form Wash upside-down for 10 min and right-side up for 10 min. Finally, it was cured in the Form Cure at the standard time and temperature for the Tough 2000 resin.

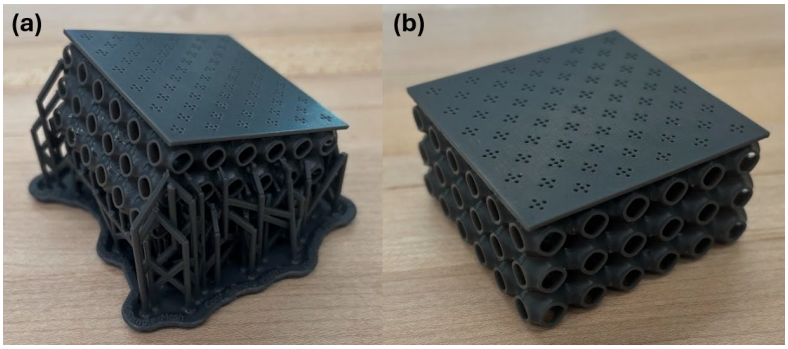

Figure 9. (a) The printed liner core with supports and (b) the printed liner core without supports.

Manual Measurement Pipeline Execution

Using the representative liner core, the manual measurement pipeline was executed. The first stage was to gather the measurements that were found using calipers. The face sheet thickness was measured 12 times for a total of 48 measurements. On each side, six measurements were aligned with the endo pores of the lattice, and the remaining six measurements were aligned with the exo pores. During this process, it was found that the face sheet thickness where the lattice connected to the face sheet was slightly thicker than the thickness aligned with the exo pores. This was most likely due to small amounts of excess resin that gathered around the connection points leading to small fillets instead of sharp edges. The unit cell size was measured in the side length, side depth, and bottom length orientations as shown in Figure 10. Based on the geometry of the lattice, a total of 60 measurements were captured for the side length orientation, 48 for the side depth orientation, and 60 for the bottom length orientation. The last measured variable was the wall thickness of the lattice. Figure 10 also shows how these measurements were collected similar to the cell size, with 144 measurements captured for each of the three orientations.

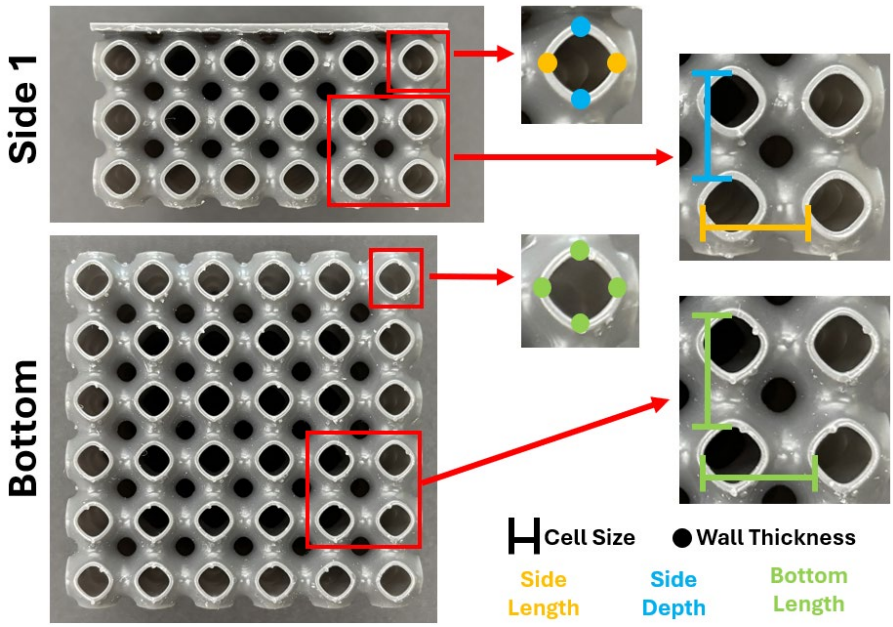

Figure 10. Measurement locations and directions for each cell size and wall thickness orientation.

Once the face sheet thickness, cell size, and wall thickness had been measured with calipers, the rest of the measurements were found using image processing tools, starting with perforation diameters. Figure 11 shows a comparison between the original image opened in ImageJ and the thresholded image used for the area estimations on the perforations. Using the thresholded image, particle analysis yielded 459 area measurements. The effective diameters of the particles were found by converting the areas to diameters using simple circle geometry. In some perforations, small flakes can be seen partially blocking the openings. This was suspected to be small contaminants from the shared Form Wash which got stuck during the wash process. The flakes caused some of the perforations to appear partially blocked or split into multiple sections in the thresholded image. After removing the diameters of both noise particles and significantly blocked/split perforations, the data were reduced to 297 effective diameters. The particle analysis also outputs a total area which was used as the total open area of the face sheet. By dividing the open area by the as-printed cross-sectional area of the face sheet, found by measuring the length and width of the face sheet, which was 51.3 mm and 50.03 mm respectively, the manufactured POA was found.

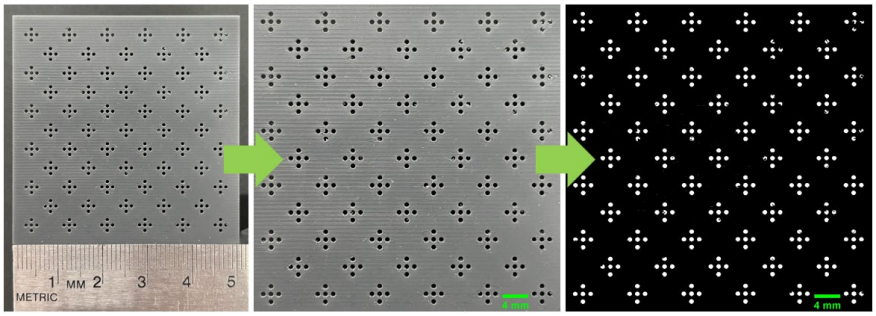

Figure 11. Facesheet image preparation for perforation area measurements.

The final design parameter measured was the isovalue. Images of the sides and bottom of the sample were run through the Canny edge detection software and cleaned in ImageJ so that a section of the endo and exo pore areas could be measured in terms of pixels as shown in Figure 12. The endo pore area was then divided by the exo pore area to find the ratio between the two and could then be related to an isovalue. Through a similar measurement technique of the ideal nTop model at several different isovalues, the relationship was found between the endo/exo pore area ratio and the isovalue. This relationship was then used to convert the manufactured pore ratios into isovalues. By analyzing each of the sides and the bottom of the sample, a total of 65 pore area ratios, and thus isovalues, were measured.

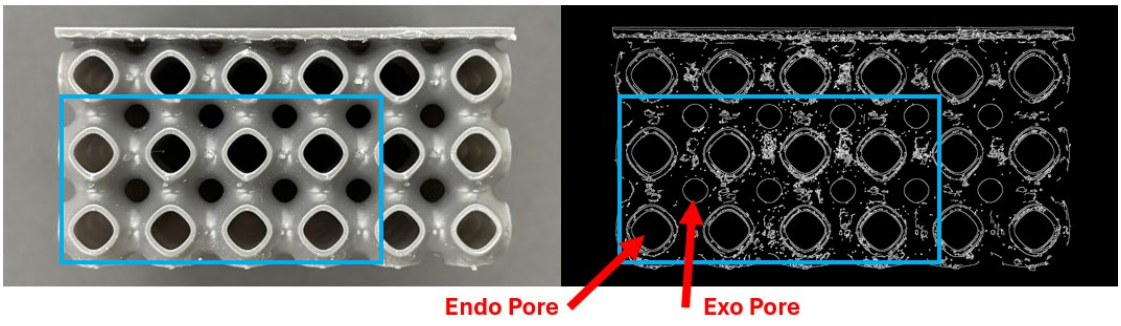

Figure 12. Conversion of lattice to binary edges for the purpose of measuring the areas of the endo and exo pores outlined in blue.

All of the collected data were used to find the average, standard deviation, minimum, and maximum values for each design variable as shown in Table 4. As can be seen, every design variable except perforation diameter and POA was found to be slightly oversized on average. This shows that most of the design variables would need to be undersized before printing in order to achieve the correct nominal dimensions in the manufactured part. Conversely, the perforation diameter and POA would need to be slightly oversized before printing. In the event that visual inspection of the distributions of the data is needed, the collected raw data can also be used to create histograms for several design variables.

Table 4. Summary of design parameter measurements.

Parameter	Nominal	Average	Standard Deviation	Minimum	Maximum
Face Sheet Thickness	1 mm	1.17 mm	0.05 mm	1.09 mm	1.29 mm
Unit Cell Size (Side Length)	8.47 mm	8.51 mm	0.04 mm	8.43 mm	8.61 mm
Unit Cell Size (Side Depth)	8.47 mm	8.51 mm	0.05 mm	8.42 mm	8.59 mm
Unit Cell Size (Bottom Length)	8.47 mm	8.50 mm	0.04 mm	8.42 mm	8.59 mm
Wall Thickness (Side Length)	0.6 mm	0.64 mm	0.03 mm	0.55 mm	0.71 mm
Wall Thickness (Side Depth)	0.6 mm	0.73 mm	0.05 mm	0.64 mm	0.87 mm
Wall Thickness (Bottom Length)	0.6 mm	0.63 mm	0.04 mm	0.55 mm	0.72 mm
Perforation Diameter	0.8 mm	0.69 mm	0.02 mm	0.64 mm	0.72 mm
Percent Open Area (POA)	5.94%	4.26%	N/A	N/A	N/A
Isovalue	0.2	0.201	0.003	0.192 mm	0.207 mm

Milestones

- Established a method for identifying geometric variations in as-manufactured TPMS lattice structures.
- Demonstrated the use of manual measurements to capture liner variation.
- Specified an approach to formulate error distributions in a way that can later be integrated with HyperStudy.

Major Accomplishments

- Quantified the presence of oversized/undersized features in manufactured TPMS liners.
- Measured a range of different design parameters through the use of manual calipers.
- Identified the need to account for both predictable build error and stochastic build error.

Publications

Windows, J., Packer, A., Nelson, E., Chowaniec, J., Mendoza, J., Reimann, C. A., Winkler, J., Homma, K., & Meisel, N. A. (2025). Identification of Stochastic Manufacturing Defects Within Additively Manufactured Acoustic Liners. *Proceedings of the Annual International Solid Freeform Fabrication Symposium*, in press.

Outreach Efforts

None.

Awards

None.

Student Involvement

Joseph Windows, an MS student in mechanical engineering, was involved in this task. He worked to identify key manufacturability challenges and determine a systematic way by which to measure and account for them in the design of the TPMS liner structures.

Plans for Next Period

- Using the systematic approach developed in this period, combine the measured findings with HyperStudy to predict acoustic performance variation based on the likelihood of stochastic error in manufactured specimens.
- Augment the measurement process using Rapidminer® machine learning software.

® Rapidminer is a registered trademark of Rapidminer, Inc., Troy, Michigan.

Task 3 – Automating the Generation of Acoustic Lattice Meshes

The Pennsylvania State University, Cornerstone Research Group

Objective

The objective of this task is to develop a tool which is capable of generating mesh structures for TPMS lattice geometries that will be integrated into the acoustic modeling procedure used in Task 1.

Research Approach

Through efforts in this task, CRG has developed a workflow for the existing acoustic modeling and analysis pipeline that will allow the user to generate a multi-cell lattice structure using the Schwarz P TPMS geometry. The workflow is outlined as follows:

Step 1. User will generate a user input file.
Step 2. Code will read in the user input file.
Step 3. Code will generate the core of a single cell TPMS structure by solving the TPMS equation at the core.
Step 4. Code will generate a thickness for a single cell by computing the core's surface normal and extrapolating the nodes outward from the core.
Step 5. Code will copy the single cell throughout the region to form the multi-cell structure.
Step 6. Code will export the single and multi-cell structures as either surface or volume mesh formats depending on the user inputs.

Currently the code is capable of generating the solid domain for a multi-cell Schwarz P TPMS structure. The overall lattice is then generated to fit within a 3D rectangular domain based on the user input parameters. The meshing algorithm itself takes advantage of the structured equation defining the TPMS geometry and is capable of generating eight structured meshes representing the eight octants of a single cell. The algorithm then stitches the eight regions to generate the single cell. At the time of this report, the user can control the approximate number of nodes making up a single cell, the sizing of a single cell, and the number of cells within each lattice structure. Figure 13 displays an example of a uniform Schwarz P lattice structure with a single-cell structure and a multi-cell structure. CRG's code can export the mesh representing the lattice structure into four formats: (1) NASTRAN, (2) Tecplot, (3) PLY, and (4) STL. The NASTRAN and Tecplot formats are volume mesh formats that can be used for computational fluid dynamics (CFD) or finite element analysis. The PLY and STL are surface mesh formats which can be used for applications such as additive manufacturing.

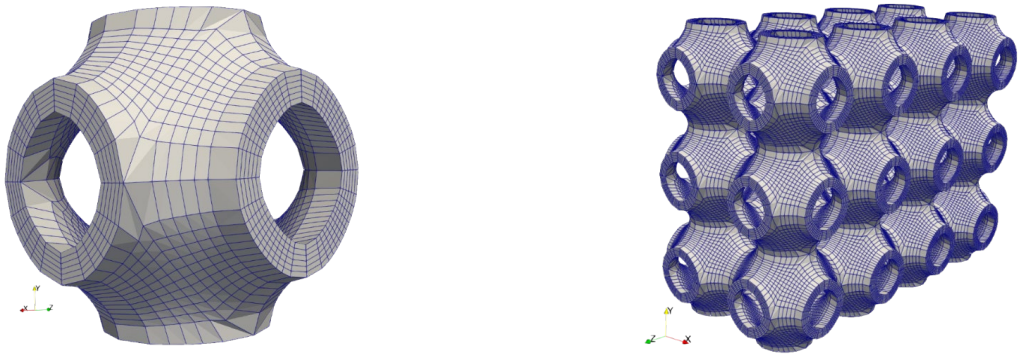

a) Single-cell structure b) Multi-cell structure

Figure 13. Single and multi-cell structures of the Schwarz P solid domain geometry generated by CRG's code.

In the latest version of the meshing tool, CRG has implemented an algorithm to generate the fluid domain of the Schwarz P structure for CFD and acoustic modeling. CRG initially utilized a similar approach to that of the solid domain generation; however the mesh quality was generally weaker, and bugs existed that prevented the mesh from being read into the modeling tool, COMSOL. Illustrations of the mesh are shown in Figure 14. CRG is currently implementing an incremental insertion algorithm that meets the Delauney criteria which helps maximize the quality of a given mesh using tetrahedrons. CRG has implemented a version of the incremental insertion algorithm in a code written for another tool developed by CRG. Modifications are being performed to the code to handle the Schwarz P TPMS geometry.

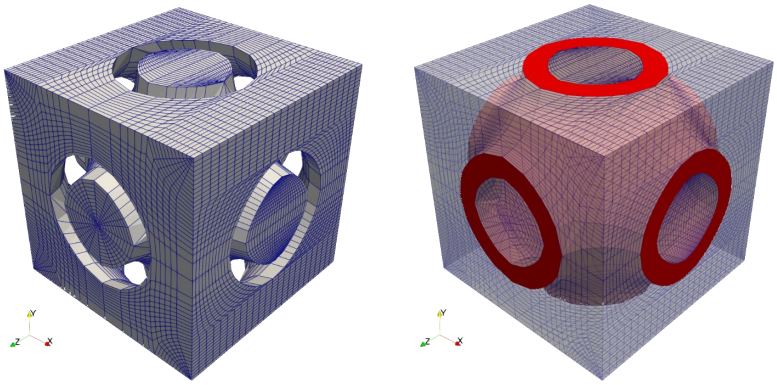

Figure 14. Single-cell structures of the Schwarz P fluid domain geometry generated by CRG's code.

In the meantime, CRG has generated and provided Penn State with a licensed executable of an alpha version of the code that can be run on the university computer systems. The provided alpha version is only capable of generating the solid domain of the mesh and only includes the four mesh formats described above as export options. Penn State has successfully generated and imported a NASTRAN version of the mesh into COMSOL using the provided code.

Milestones

- Demonstrated the use of direct mesh modeling to generate multi-cell solid TPMS domains.
- Established a method to export the generated meshes for use in existing acoustic simulation.

Major Accomplishments

- Created a tool capable of generating both solid and fluid domains suitable for acoustic analysis.

Publications

None

Outreach Efforts

None.

Awards

None.

Student Involvement

None

Plans for Next Period

- Continue to work on improving the implementation of the fluid domain generation for the Schwarz P TPMS geometry.
- Once a reasonable fluid domain is generated, send a sample mesh over to Penn State in the NASTRAN format to verify that it can be read into their version of COMSOL.
- Initiate the expansion of the code to generate the fluid domain representation of a multi-cellular Schwarz P geometry.
- Exported the multi-cellular geometry in a suitable format such as NASTRAN and provided to Penn State for testing in COMSOL.